European Radiology (2019) 29:3658–3668
https://doi.org/10.1007/s00330-019-06019-9

CARDIAC

Quantification of myocardial deformation by deformable registration–based analysis of cine MRI: validation with tagged CMR

Mariana M. Lamacie[1] · Christian P. Houbois[1,2] · Andreas Greiser[3] · Marie-Pierre Jolly[4] · Paaladinesh Thavendiranathan[1,5] · Bernd J. Wintersperger[1,2]

Received: 20 October 2018 / Revised: 5 December 2018 / Accepted: 18 January 2019 / Published online: 15 February 2019

Abstract

Objectives To validate deformable registration algorithms (DRAs) for cine balanced steady-state free precession (bSSFP) assessment of global longitudinal strain (GLS) and global circumferential strain (GCS) using harmonic phase (HARP) cardiovascular magnetic resonance as standard of reference (SoR).

Methods Seventeen patients and 17 volunteers underwent short axis stack and 2-/4-chamber cine bSSFP imaging with matching slice long-axis and mid-ventricular spatial modulation of magnetization (SPAMM) myocardial tagging. Inverse DRA was applied on bSSFP data for assessment of GLS and GCS while myocardial tagging was processed using HARP. Intra- and inter-observer variability assessment was based on repeated analysis by a single observer and analysis by a second observer, respectively. Standard semi-automated short axis stack segmentation was performed for analysis of left ventricular (LV) volumes and ejection fraction (EF).

Results DRA demonstrated strong relationships to HARP for myocardial GLS ($R^2 = 0.75$; $p < 0.0001$) and endocardial GLS ($R^2 = 0.61$; $p < 0.0001$). GCS result comparison also demonstrated significant relationships between DRA and HARP for myocardial strain ($R^2 = 0.61$; $p < 0.0001$) and endocardial strain ($R^2 = 0.51$; $p < 0.0001$). Both methods demonstrated small systematic errors for intra- and inter-observer variability but DRA demonstrated consistently lower CV. Global LVEF was significantly lower ($p = 0.0099$) in patients (53.7%; IQR 43.9/64.0%) than in healthy volunteers (62.6%; IQR 61.1/66.2%). DRA and HARP strain data demonstrated significant relationships to LVEF.

Conclusions Non-rigid deformation method–based DRA provides a reliable measure of peak systolic GCS and GLS based on cine bSSFP with superior intra- and inter-observer reproducibility compared to HARP.

Key Point

- *Myocardial strain can be reliably analyzed using inverse deformable registration algorithms (DRAs) on cine CMR.*
- *Inverse DRA-derived strain shows higher reproducibility than tagged CMR.*
- *DRA and tagged CMR-based myocardial strain demonstrate strong relationships to global left ventricular function.*

Keywords Magnetic resonance imaging, cine · Algorithms · Ventricular function, left · Myocardium

✉ Bernd J. Wintersperger
Bernd.Wintersperger@uhn.ca

[1] Department of Medical Imaging, University Health Network, 1 PMB-273, 585 University Avenue, Toronto, Ontario M5G 2N2, Canada

[2] Department of Medical Imaging, University of Toronto, Toronto, Ontario, Canada

[3] Siemens Healthcare GmbH, Erlangen, Germany

[4] Siemens Healthcare AG, Medical Imaging Technologies, Princeton, NJ, USA

[5] Department of Medicine, Division of Cardiology, University of Toronto, Toronto, Ontario, Canada

Abbreviations

BSA	Body surface area
bSSFP	Balanced steady-state free precession
CMR	Cardiovascular magnetic resonance
CV	Coefficient of variation
DENSE	Displacement encoding with stimulated echoes
DRA	Deformable registration algorithms
EDV	End-diastolic volume
EF	Ejection fraction
ESV	End-systolic volume
FLASH	Fast low angle shot
FT	Feature tracking

GCS	Global circumferential strain
GLS	Global longitudinal strain
GRAPPA	Generalized autocalibrating partial parallel acquisition
GRS	Global radial strain
HARP	Harmonic phase
IQR	Interquartile range
LV	Left ventricle
LVEF	Left ventricular ejection fraction
MASS	Myocardial mass
REB	Research Ethics Board
SENC	Strain encoded
SoR	Standard of reference
SPAMM	Spatial modulation of magnetization
SV	Stroke volume
TPM	Tissue phase mapping

Introduction

Besides being considered the standard of reference (SoR) for quantification of ventricular volumes and global systolic function, cardiovascular magnetic resonance (CMR) is also known as a highly accurate approach to regional function and deformation assessment [1–5]. While left ventricular ejection fraction (LVEF) has demonstrated prognostic implications in various cardiac pathologies, measurable deterioration of LVEV may only occur rather late in the disease process [6]. Changes in regional function and myocardial deformation have been shown to provide more sensitive identification of functional abnormalities at earlier stages than LVEF with prognostic and therapeutic importance [2, 7].

Various dedicated CMR approaches for assessment of myocardial deformation and strain, such as myocardial tagging [8, 9], strain-encoded MRI (SENC) [10], displacement encoding with stimulated echoes (DENSE) [11], and tissue phase mapping (TPM) [12], have been developed and evaluated. Despite further improvements in data acquisition and ease in processing (e.g., harmonic phase magnetic resonance imaging, HARP), none of these techniques have been incorporated into clinical routine CMR [13–15].

With the development of feature-tracking (FT) algorithms, assessment of myocardial deformation and strain based on routine cine balanced steady-state free precession (bSSFP) data has recently gained attraction [16, 17]. Underlying techniques have been vastly described in the literature and, with some exceptions, comparison to myocardial tagging have demonstrated good levels of agreement [18–21]. However, tracking algorithms of most commercially available software solutions are not openly accessible ("black box" approaches), as such limiting insight from operators and reengineering for standardization purposes.

As an alternative method to FT algorithms, deformable registration–based analysis (DRA) tools, originally aimed at motion correction, have been described for strain assessment combining automated/semi-automated cine bSSFP segmentation with deformation field calculation [22–24]. Studies have demonstrated superior intra- and inter-observer reproducibility of DRA in comparison to FT approaches and also indicated diagnostic benefit in longitudinal follow-up of therapy management [22, 23, 25].

To the best of our knowledge, DRA has not yet been validated against an accepted standard of reference technique for CMR strain evaluation.

We hypothesize that DRA-based strain assessment based on cine bSSFP data provides accurate and reproducible measures of myocardial strain. The aim of the present study therefore was to validate DRA assessment of global longitudinal strain (GLS) and global circumferential strain (GCS) with harmonic phase (HARP) CMR serving as SoR.

Materials and methods

Study population

The patient study was designed as a prospective cohort study. Seventeen patients (43.0 years old; IQR, 27.5/49.3 years old; m/f = 10/7) referred to clinical CMR for suspicion of/known cardiac disease were consecutively enrolled into the study. Referral diagnosis included non-ischemic cardiomyopathies ($n = 10$), inflammatory heart disease ($n = 3$), ischemic cardiomyopathy ($n = 1$), valvular heart disease ($n = 1$), and repaired congenital heart disease ($n = 2$).

A separate cohort of 17 healthy volunteers (47.0 years old; IQR, 35.8/64.3 years old; m/f = 5/12) were prospectively included. These participants were enrolled as part of the healthy volunteer arm of the ongoing EMBRACE-MRI trial (NCT02306538) and were free of cardiovascular disease or cardiovascular risk factors.

The study has been approved by the Research Ethics Board (REB) and all study participants provided written informed consent.

Detailed cohort information is provided in Table 1.

Magnetic resonance imaging

CMR was performed at 1.5 Tesla (MAGNETOM Avanto fit, Siemens Healthineers). In all instances, the imaging protocol included multiplanar cine bSSFP techniques applied in multiple long-axes orientations (2-/4-chamber) and a stack of parallel short axes slices for ventricular coverage from base to apex. Cine bSSFP was acquired in 8-mm slice thickness (2-mm gap for short axis) and all slice planning was performed using semi-automated planning support for consistency.

Myocardial tagging was performed in 2-/4-chamber orientation and at a mid-ventricular short axis orientation using spatial modulation of magnetization (SPAMM) prepared fast low angle shot (FLASH) cine imaging. Slice positions were matched to respective cine bSSFP orientations (Fig. 1). Detailed sequence parameters are provided in Table 2.

Image analysis

Ventricular function analysis

Analysis of global LV volumetric and functional parameters was performed by a single observer (M.M.L.) using a commercially available software package (MEDIS Suite 2.3., MEDIS). The following parameters were measured: end-diastolic volume (EDV), end-systolic volume (ESV), stroke volume (SV), ejection fraction (EF), and myocardial mass (MASS). All volumes were indexed to the patient's body surface area (BSA).

Strain analysis

Inverse deformable registration algorithm Acquired 2-/4-chamber long-axis cine as well as a single slice of short axis (slice location matching to tagging acquisition) cine bSSFP data was transferred to an offline workstation for further processing. Inverse DRA was based on a prototype automated segmentation tool programmed in Visual C++ (Trufi Strain, Siemens Healthineers, Medical Imaging Technologies). The detailed algorithm and approaches to data processing have been described previously [22, 25].

Myocardial tagging All acquired tagging data sets were transferred to an offline workstation and analyzed using a commercially available post-processing tool (HARP, Myocardial Solutions). Processing required contouring on an initial phase by placing markers along the endo- and epicardial borders that are then automatically propagated across all phases of the same slice. Following adjustment in the raw data domain, the software calculates displacement maps based on identification of harmonic peaks in the frequency domain of tagging data with their respective phase changes over time [26, 27].

Strain results for individual long-axis longitudinal strain as well as for global circumferential strain were transferred for further analysis.

Intra-/inter-observer agreement analysis For the purpose of intra-observer agreement analysis, all data sets were re-analyzed using both algorithms, inverse DRA and HARP, by observer 1 with a 4-week minimum interval blinded to results of the first analysis.

For the purpose of inter-observer agreement analysis, both inverse DRA strain analysis and HARP strain analysis were performed by two observers (M.M.L., C.P.H.) blinded to all clinical information and each other's measurements.

General strain definitions For both approaches, peak systolic GCS was defined as the maximal circumferential strain (for the entire circumference of the acquired slice) within systole (visually defined by minimum LV volume). For peak systolic GLS, respective peaks of individual axes (2ch and 4ch) values were averaged.

From both methods, strain data was reported separately for myocardial strain (entire wall thickness) as well as endocardial strain (endocardial 3rd of the wall thickness).

Based on the nature of the applied analysis techniques, all DRA results are reported as Lagrangian strain while HARP results are reported in Eulerian (Natural) strain. These definitions relate to a difference in the frame of reference [28].

Statistical analysis

Continuous variables are reported as median and IQR unless stated otherwise. All strain data are reported in percentages. Assessment of normal distribution was performed using the Kolmogorov-Smirnov test. Comparison of baseline data between patients and volunteers was performed using Student's t test for independent samples or a Mann-Whitney test as appropriate. Comparison of individual strain values between both methods was performed using Student's t test for paired samples or a Wilcoxon signed-rank test and intra-method comparison between patients and volunteers employed Student's t test for independent samples or the Mann-Whitney test as appropriate. Assessment of the degree of association between both methods and the relationship of individual strain data to global functional parameters was performed using linear regression analysis.

For assessment of systematic and random error in repeated evaluations (intra-/inter-observer), Bland-Altman analysis was employed. For assessment of intra-observer and inter-observer agreement, calculation of the coefficient of variation (CV) was performed. Statistical comparison of coefficients of variation was performed using an F-test.

All statistical analysis was performed using MedCalc® (Version 17.2, MedCalc Software bvba) and statistical significance was assumed at $p < 0.05$.

Results

Global LV parameters

Comparison of global LV parameters demonstrated a significantly lower median LVEF (53.7%; range, 16.2–77.1%) in the patient population as compared to the healthy volunteer

Table 1 Patient demographics and characteristics

	Total ($n = 34$)	Patients ($n = 17$)	Volunteers ($n = 17$)	
General				
Age (year)	46.0 [35.0, 57.0]	43.0 [27.5, 49.3]	47.0 [35.8, 64.3]	$p = 0.084$
Gender (m/f)	15/19	10/7	5/12	n.a.
BSA (m^2)	1.82 [1.63, 2.01]	1.84 [1.68, 2.02]	1.75 [1.60, 2.02]	$p = 0.588$
Global LV parameters				
LV EF (%)	61.3 [53.7, 66.0]	53.7 [43.9, 64.0]	62.6 [61.1, 66.2]	$p < 0.01$
LV EDVi (mL/m^2)	81.3 [74.7, 98.6]	83.0 [73.2, 118.1]	79.6 [76.8, 91.9]	$p = 0.760$
LV ESVi (mL/m^2)	31.4 [27.1, 38.5]	35.4 [27.9, 55.6]	29.3 [26.7, 34.8]	$p = 0.131$
LV MASSi (g/m^2)	51.2 [42.6, 68.2]	68.2 [50.1, 97.5]	47.0 [39.9, 51.0]	$p = 0.001$

Data (except gender) is presented in median [IQR]

population (62.6%; range, 57.7–80.0%) ($p < 0.01$). Furthermore, the patients' median LV MASSi was significantly higher than that in volunteers ($p = 0.001$). No significant differences were identified for LV EDVi and LV ESVi. Details of the population are shown in Table 1.

Myocardial strain

Feasibility

Cine bSSFP and tagging-based strain post-processing and evaluation were feasible in all 34 cases (100%). In general, DRA analysis does not require any correction of segmentation and as such generation of strain results was less time-consuming than HARP. An overview of all strain results is provided in Table 3.

Global longitudinal strain

Cine bSSFP DRA analysis-based myocardial GLS (− 14.3; IQR, − 16.6/− 11.4) was significantly lower than HARP-based myocardial GLS (− 13.3; IQR, − 14.6/− 9.5; $p < 0.001$) but results of DRA demonstrated a strong relationship to HARP data ($R^2 = 0.75$ $p < 0.0001$) (Table 3) (Fig. 2a). For endocardial GLS data, DRA (− 14.4; IQR, − 16.4/− 11.8) did not differ from HARP (− 13.7; IQR, − 16.0/− 10.5); $p = 0.078$) and again there was a strong association between the two techniques ($R^2 = 0.61$; $p < 0.0001$) (Table 3) (Fig. 2b).

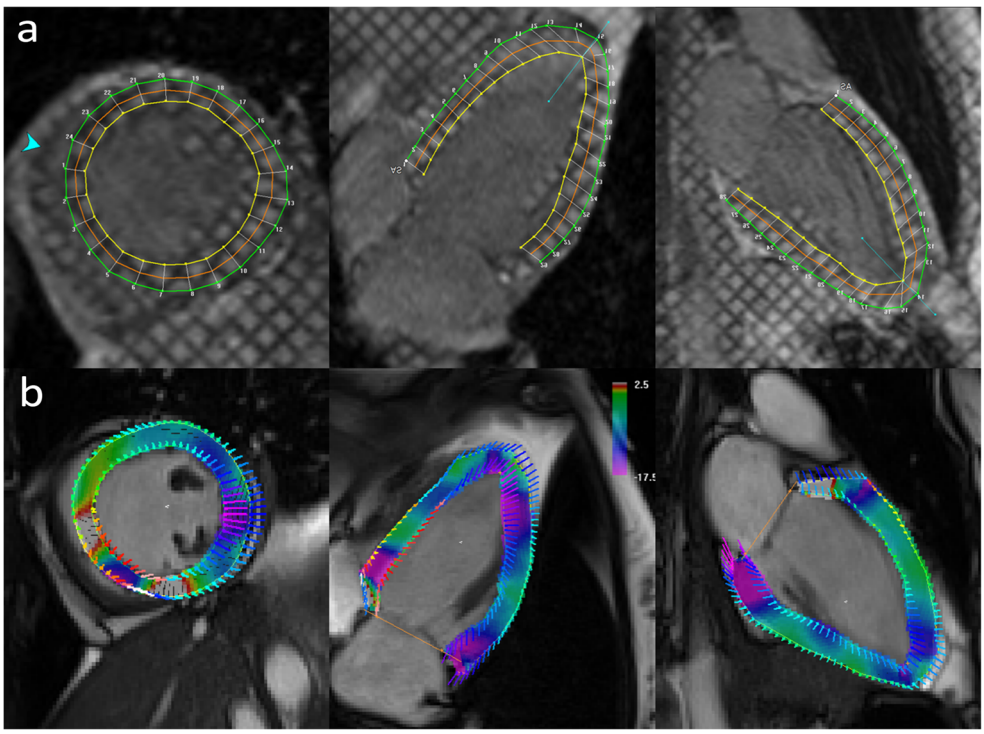

Fig. 1 Matching short axis, 4-chamber/2-chamber view slice locations/orientations for (**a**) myocardial tagging (SPAMM) and (**b**) cine bSSFP used for analysis with HARP and DRA, respectively

Table 2 Details of performed sequence techniques for strain assessment

	Cine bSSFP	SPAMM tagging
Repetition time (TR)	2.8 ms	8.1 ms
Echo time (TE)	1.2 ms	3.9 ms
Flip angle	70 degrees	14 degrees
Parallel imaging	GRAPPA $R = 2$	GRAPPA $R = 2$
Temporal resolution (Tres)	36 ms	41 ms
Slice thickness	8 mm	8 mm
Pixel size	1.6×1.6 mm^2	1.4×1.4 mm^2
Other		Grid tagging; 8-mm tag distance

Global circumferential strain

For GCS results across the entire myocardium, there was no significant difference in strain values between DRA (− 14.3; IQR, − 15.8/− 12.3) and HARP (− 14.3; IQR, − 15.7/− 11.2; $p = 0.0182$) with a strong relationship between both methods ($R^2 = 0.61$; $p < 0.0001$) (Table 3) (Fig. 2a). The endocardial GCS analysis revealed significantly lower values for DRA (− 20.2; IQR, − 22.2/− 16.8) than for HARP (− 16.1; IQR, − 18.8/− 13.8; $p < 0.001$) and results demonstrated a good relationship to each other ($R^2 = 0.51$ $p < 0.0001$) (Table 3) (Fig. 2b).

Intra-/inter-observer agreement

For all repeated analyses by a single observer (intra-observer), Bland-Altman evaluations demonstrated small systematic bias for both methods. However, for all evaluated strain parameters, DRA demonstrated substantially narrower limits of agreement (Table 4) (Fig. 3). Furthermore, DRA demonstrated significantly lower coefficients of variation (CV) than HARP analysis as a measure for intra-observer agreement across all evaluated parameters (1.6–3.7% vs. 6.6–9.3%; all $p < 0.01$) (Table 4).

The repeated analysis by a second observer for the purpose of inter-observer agreement demonstrated a larger systematic bias for HARP analysis in all strain measures but endocardial GCS as well as substantially wider limits of agreement (Table 4) (Fig. 4). Furthermore, DRA again demonstrated significantly lower coefficients of variation (CV) than HARP analysis as a measure for inter-observer agreement for all parameters (3.6–4.7% vs. 11.1–18.0%; all $p < 0.001$) but endocardial GCS (5.6% vs. 7.0%; $p = 0.156$) (Table 4).

Relationship of strain and global left ventricular systolic function

Both DRA- and HARP-based GLS results (myocardial and endocardial) demonstrated significant relationships with LVEF (all $p < 0.001$) (Fig. 5a, b).

Table 3 Overview of results for global longitudinal (GLS) and circumferential (GCS) strain values based on inverse deformable registration analysis (DRA) and HARP techniques. Results are provided for the total cohort as well as for the patient and volunteer subgroups

		DRA Median (IQR)	HARP Median (IQR)	
GLS myocardial	Total ($n = 34$)	− 14.3 [− 16.6, − 11.4]	− 13.3 [− 14.6, − 9.5]	$p < 0.001$
	Patient ($n = 17$)	− 11.4 [− 12.9, − 9.7]$^{\&}$	− 9.5 [− 10.6, − 7.7]$^{\&}$	$p = 0.002$
	Volunteers ($n = 17$)	− 16.6 [− 17.9, − 15.2]	− 14.6 [− 17.4, − 14.1]	$p = 0.026$
GLS endocardial	Total ($n = 34$)	− 14.4 [− 16.4, − 11.8]	− 13.7 [− 16.0, − 10.5]	$p = 0.078$
	Patient ($n = 17$)	− 11.8 [− 14.3, − 10.6]$^{\&}$	− 10.9 [− 13.4, − 7.5]$^{\&}$	$p = 0.054$
	Volunteers ($n = 17$)	− 16.0 [− 16.9, − 14.8]	− 16.0 [− 17.7, − 14.0]	$p = 0.661$
GCS myocardial	Total ($n = 34$)	− 14.3 [− 15.8, − 12.3]	− 14.3 [− 15.7, − 11.2]	$p = 0.182$*
	Patient ($n = 17$)	− 12.3 [− 14.0, − 8.0]$^{\&}$	− 12.0 [− 14.3, − 9.5]$^{\&}$	$p = 0.452$
	Volunteers ($n = 17$)	− 15.8 [− 17.9, − 14.4]	− 15.6 [− 18.0, − 14.4]	$p = 0.453$
GCS endocardial	Total ($n = 34$)	− 20.2 [− 22.2, − 16.8]	− 16.1 [− 18.8, − 13.8]	$p < 0.001$*
	Patient ($n = 17$)	− 16.8 [− 20.7, − 12.9]$^{\&}$	− 14.5 [− 17.4, − 13.0]$^{\&}$	$p = 0.040$*
	Volunteers ($n = 17$)	− 20.7 [− 22.6, − 20.0]	− 16.9 [− 19.9, − 15.8]	$p = 0.002$*

Data is presented in median [IQR]; $^{\&}$ $p < 0.05$ in comparison to healthy volunteers (same method); *Wilcoxon signed-rank test

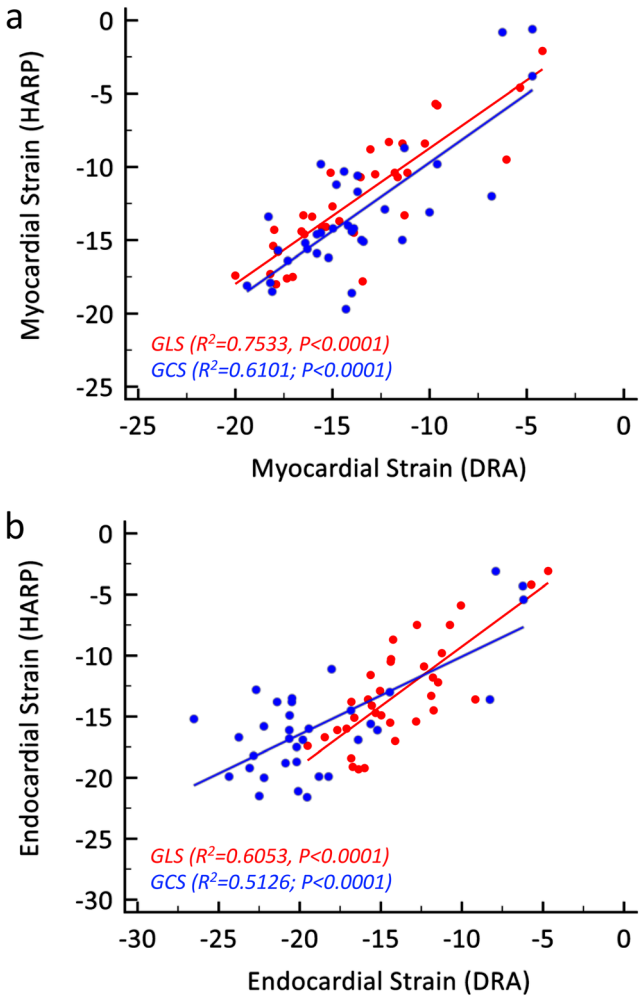

Fig. 2 Relationship between DRA and HARP for both (**a**) myocardial strain (GLS, GCS) and (**b**) endocardial strain (GLS, GCS) for all subjects

Similar findings are shown for DRA- and HARP-derived GCS data (myocardial and endocardial), with all values demonstrating significant relationships to LVEF (all $p < 0.001$) (Fig. 5c, d).

Discussion

Our study demonstrates that DRA-based algorithms applied to cine bSSFP images provide global longitudinal and circumferential strain results that strongly correlate to measurements obtained using HARP-based analysis of tagged CMR. Furthermore, repeated analysis confirms a significantly lower intra- and inter-observer variability for DRA compared to HARP. To the best of our knowledge, this is the first study to report DRA results with HARP as standard of reference for both longitudinal and circumferential strain information.

While myocardial strain assessment in routine echocardiography has recently become available, dedicated CMR imaging techniques have not gained attraction in clinical scenarios while commonly being applied in research settings. This is most likely attributed to the need for dedicated data acquisitions resulting in extended scan times. Contrary to dedicated approaches in CMR (e.g., tagging, SENC, DENSE, TPM), cine bSSFP-based approaches rely on data acquired as part of the assessment of global cardiac function [16]. This has renewed the interest in assessment of myocardial deformation and strain assessment in a clinical setting.

The vast majority of these approaches are based on feature tracking (FT). However, despite a large body of literature on FT-derived strain, published data on a rigorous comparison using an accepted SoR such as myocardial tagging remains

Table 4 Results of intra-observer and inter-observer comparison based on (a) Bland-Altman analysis and (b) coefficient of variation (CV)

(a)

	Bland-Altman analysis (intra-observer)				Bland-Altman analysis (inter-observer)			
	DRA		HARP		DRA		HARP	
	Bias	Limits of agreement	Bias	Limits of agreement	Bias	Limits of agreement	Bias	Limits of agreement
GLS myocardial	0.1	− 0.5; 0.7	− 0.7	− 2.8; 1.4	− 0.4	− 1.5; 0.8	− 1.9	− 6.2; 2.4
GLS endocardial	0.1	− 1.1; 1.4	− 0.3	− 2.7; 2.0	0.4	− 1.3; 2.1	− 2.0	− 6.3; 2.3
GCS myocardial	0.0	− 0.9; 0.9	− 0.9	− 3.7; 1.8	0.1	− 1.3; 1.5	− 1.3	− 4.2; 1.7
GCS endocardial	0.1	− 1.9; 2.1	− 0.1	− 3.4; 3.3	− 0.8	− 3.2; 1.6	− 0.2	− 3.2; 2.9

(b)

	CV (%) (intra-observer)			CV (%) (inter-observer)		
	DRA	HARP	Significance	DRA	HARP	Significance
GLS myocardial	1.6	7.6	$p < 0.001$	3.6	18.0	$p < 0.001$
GLS endocardial	3.3	6.6	$p = 0.002$	4.7	17.3	$p < 0.001$
GCS myocardial	2.3	9.3	$p < 0.001$	3.6	11.1	$p < 0.001$
GCS endocardial	3.7	7.7	$p = 0.002$	5.6	7.0	$p = 0.156$

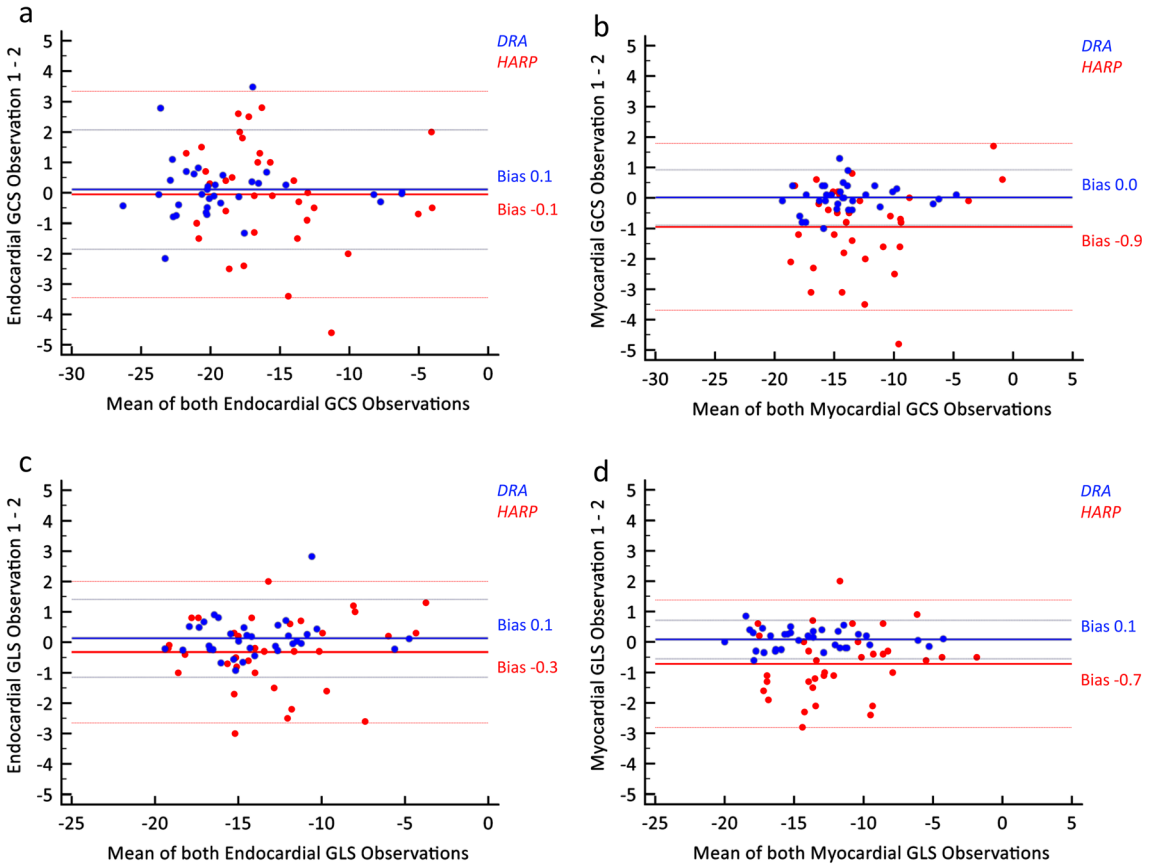

Fig. 3 **a**–**d** Comparative Bland-Altman analysis for repeated analysis (intra-observer) of strain data with DRA and HARP

sparse. In a small subset ($n = 20$) of a volunteer study, reasonably good levels of agreement of FT to myocardial tagging were reported for circumferential strain while such levels were not achieved for longitudinal and radial strain measures [21]. Other studies have demonstrated mixed results regarding the correlation of FT-derived strain to HARP analysis with the largest cohort study by Hor et al reporting a high correlation of mid-ventricular circumferential FT strain to HARP data [29, 30].

All of the above studies applied the same commercially available FT software algorithm. A small volunteer study on inter-vendor comparison demonstrated that results vary based on the applied commercially available algorithms [31, 32]. Most recently, Barreiro-Pérez et al [33] have confirmed such variations stating that despite excellent intra- and inter-observer reproducibility, results for GLS and GRS are not interchangeable between different FT algorithms. This highlights the problem of implementations of algorithms in quantitative imaging that are not accessible in its entirety to the public ("black box" approaches).

Besides accuracy of results, reproducibility is of high importance. HARP analysis has been reported to result in low intra-observer and inter-observer variability for circumferential strain analysis [27, 34]. Furthermore, approaches using myocardial tagging demonstrate better intra-/inter-observer agreement in circumferential strain assessment than FT [29, 30, 35]. Feisst et al [35] also demonstrated that the reliability of FT results is to a higher degree dependent on user experience. DRA has recently been reported superior to FT in intra-/inter-observer agreement [22]. The current study confirms the excellent intra-observer agreement of automated/semi-automated DRA and as such also confirms the results of recent studies conducted by Keller et al and Jolly et al [23, 25]. The direct comparison of DRA and HARP in the current study demonstrates that DRA has a significantly lower intra-observer variability than HARP for both circumferential and longitudinal global systolic strains with additionally substantially lower random error in repeated analysis (Table 4) (Fig. 3).

While for all aspects of DRA-based results a significant relationship to HARP results has been demonstrated (Fig. 2), direct comparison with HARP also demonstrated some significant differences in absolute values. DRA data for myocardial GLS as well as data for endocardial GCS were significantly lower than respective HARP results. These differences apply to the total study population as well as across the patient and volunteer subgroups (Table 3). Fairly similar differences

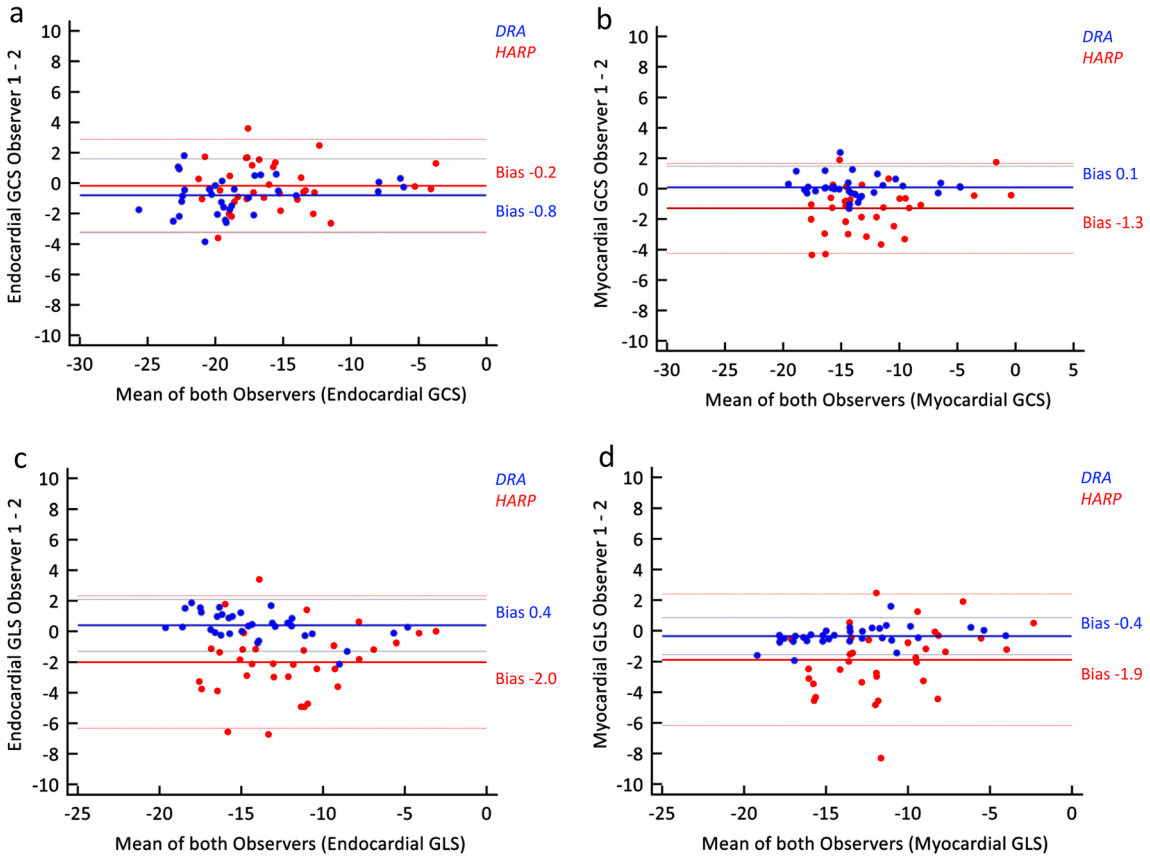

Fig. 4 **a**–**d** Comparative Bland-Altman analysis for repeated analysis (inter-observer) of strain data with DRA and HARP

between DRA and HARP have recently been reported by Jolly et al [25] in a longitudinal chemotherapy study. Possible reasons for this finding include potential minor variations in slice position dependent on the subjects' respiratory levels in consecutive breath-holds. Furthermore, bSSFP cine based algorithms tend to focus on "features" along high-contrast interfaces such as the endocardial/blood border while tagged CMR provides pan-myocardial assessment of motion. Very likely, the consistently lower (more negative) DRA results also relate to the different frame of reference of reported strain results (Lagrangian vs. Eulerian). While HARP provides highly automated processing for faster analysis, this fast-tracking method is predominately limited to Eulerian strain with knowingly less extreme values compared to the Lagrangian equivalent [28, 36]. However, as not all strain data demonstrated significant differences between both methods, variations in the approach to strain computation (including algorithm differences) may also have contributed. Such differences generally also explain result differences among different CMR FT algorithms.

Beyond these described differences in absolute strain values, results of both approaches, DRA and HARP, demonstrated a significant relationship to global LVEF (Fig. 4). As for endocardial GCS, this relationship to EF was significantly higher for DRA than for HARP. Various studies have recently demonstrated such a relationship for DRA to measures of global LV function while literature results for HARP are not as consistent [22, 25]. While showing a significant relationship between LVEF- and DRA-based strains, Jolly et al [25] could not find such a relationship for HARP. Lu et al [29] reported various levels of relationship of HARP-based peak systolic circumferential strain to global LVEF measures; while, like in this study, at the mid-ventricular level HARP correlated significantly to LVEF for circumferential peak systolic strain, such a relationship was not present for the global (along entire ventricle) circumferential strain data.

In general, the following limitations apply to this study. The overall study cohort was limited in size ($n = 34$) and, despite covering a wide range of global LV function with different underlying pathologies in the patient population, the overall number of patients with moderate to severe LV impairment was low. Furthermore, we had opted to not include analysis of radial strain data as tagged CMR might not provide the high-level standard as it does for circumferential and longitudinal strain analysis. As documented in previous studies, large variations of peak systolic radial strain values may occur in myocardial tagging (including HARP analysis) [29, 37]. While intra- and

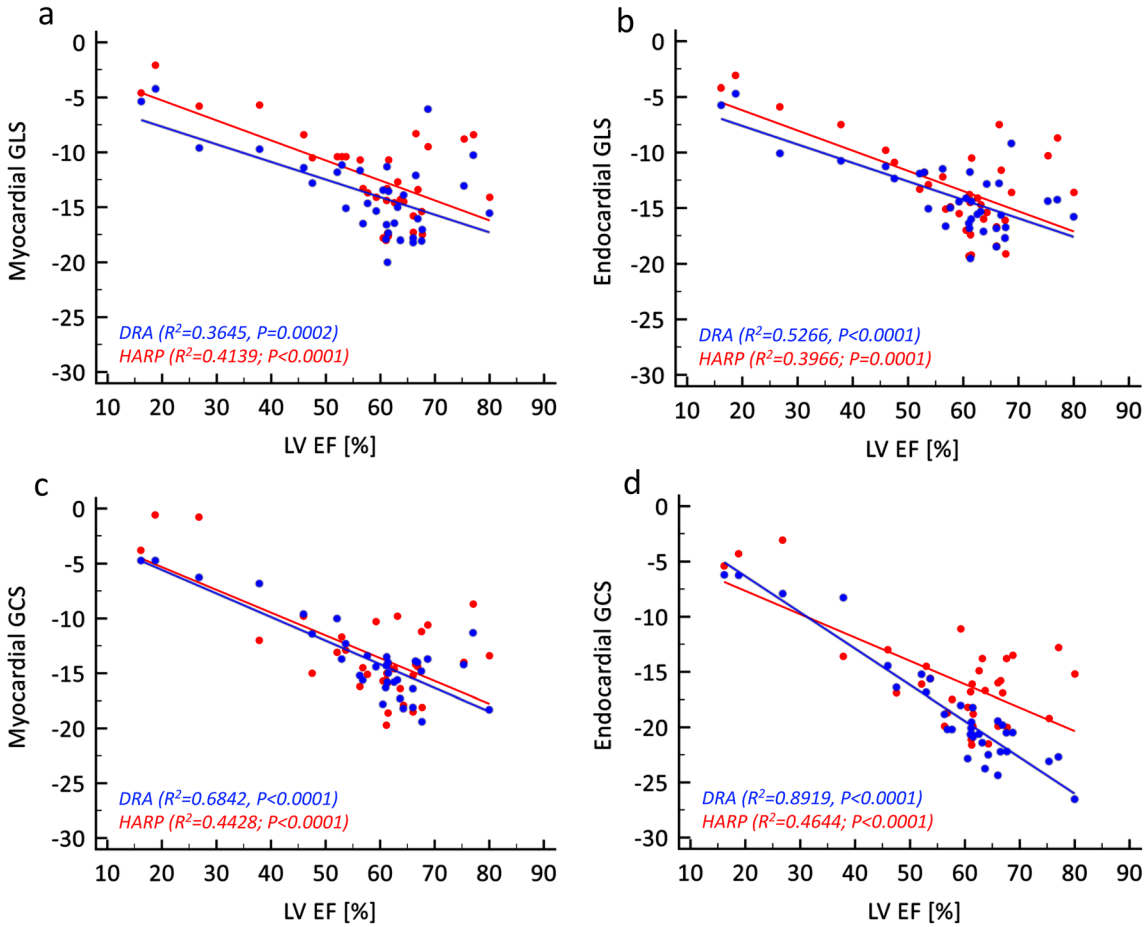

Fig. 5 **a**–**d** Relationship between global LVEF and strain results by both MR methods. Relationships are shown for (**a**) myocardial and (**b**) endocardial global longitudinal strain (GLS) as well as (**c**) myocardial and (**d**) endocardial global circumferential strain (GCS)

inter-observer variability are important measures, inter-study variability has not been assessed in this study. Further studies are required to close this gap.

Conclusion

The current study demonstrates that non-rigid deformation method-based assessment of myocardial strain using cine bSSFP images not only provides reliable measures of peak systolic global circumferential and longitudinal strain with good correlation to HARP, but also superior reproducibility to HARP. Further studies are warranted regarding the validation of DRA-based radial strain using an appropriate SoR such as DENSE. However, standardization of methods, consensus approaches, and avoidance of black box algorithms remain the most crucial aspect in pushing the envelope for clinical strain assessment in CMR.

Acknowledgments Results of this study have in part been presented at RSNA 2017 (oral presentation).

Funding The authors state that this work has not received any funding.

Compliance with ethical standards

Guarantor The scientific guarantor of this publication is Dr. Bernd J. Wintersperger.

Conflict of interest The authors of this manuscript declare relationships with the following companies:

Bernd J. Wintersperger, Research Support Siemens Healthineers

Bernd J. Wintersperger, Speakers Honorarium Siemens Healthineers

Andreas Greiser, Employee Siemens Healthineers, Erlangen, Germany

Marie-Pierre Jolly, Employee (former, at time of study) Siemens Healthineers, Medical Imaging Technologies, Princeton, NJ, USA

The study was performed under a Master Research Agreement (MRA) between the University Health Network and Siemens Healthineers.

Statistics and biometry One of the authors has significant statistical expertise (Dr. Thavendiranathan).

Informed consent Written informed consent was obtained from all subjects (patients) in this study.

Ethical approval Institutional Review Board approval was obtained.

Methodology
- prospective
- case-control study
- performed at one institution

References

1. Sanderson JE (2007) Heart failure with a normal ejection fraction. Heart 93:155–158
2. Sjøli B, Ørn S, Grenne B et al (2009) Comparison of left ventricular ejection fraction and left ventricular global strain as determinants of infarct size in patients with acute myocardial infarction. J Am Soc Echocardiogr 22:1232–1238
3. Pattynama PM, De Roos A, Van der Wall EE, Van Voorthuisen AE (1994) Evaluation of cardiac function with magnetic resonance imaging. Am Heart J 128:595–607
4. Kalam K, Otahal P, Marwick TH (2014) Prognostic implications of global LV dysfunction: a systematic review and meta-analysis of global longitudinal strain and ejection fraction. Heart 100:1673–1680
5. Mordi I, Bezerra H, Carrick D, Tzemos N (2015) The combined incremental prognostic value of LVEF, late gadolinium enhancement, and global circumferential strain assessed by CMR. JACC Cardiovasc Imaging 8:540–549
6. Solomon SD, Anavekar N, Skali H et al (2005) Influence of ejection fraction on cardiovascular outcomes in a broad spectrum of heart failure patients. Circulation 112:3738–3744
7. Smedsrud MK, Pettersen E, Gjesdal O et al (2011) Detection of left ventricular dysfunction by global longitudinal systolic strain in patients with chronic aortic regurgitation. J Am Soc Echocardiogr 24:1253–1259
8. Zerhouni EA, Parish DM, Rogers WJ, Yang A, Shapiro EP (1988) Human heart: tagging with MR imaging–a method for noninvasive assessment of myocardial motion. Radiology 169:59–63
9. Young AA, Axel L, Dougherty L, Bogen DK, Parenteau CS (1993) Validation of tagging with MR imaging to estimate material deformation. Radiology 188:101–108
10. Osman NF, Sampath S, Atalar E, Prince JL (2001) Imaging longitudinal cardiac strain on short-axis images using strain-encoded MRI. Magn Reson Med 46:324–334
11. Aletras AH, Ding S, Balaban RS, Wen H (1999) DENSE: displacement encoding with stimulated echoes in cardiac functional MRI. J Magn Reson 137:247–252
12. Codreanu I, Pegg TJ, Selvanayagam JB et al (2014) Normal values of regional and global myocardial wall motion in young and elderly individuals using navigator gated tissue phase mapping. Age (Dordr) 36:231–241
13. Osman NF, Kerwin WS, McVeigh ER, Prince JL (1999) Cardiac motion tracking using CINE harmonic phase (HARP) magnetic resonance imaging. Magn Reson Med 42:1048–1060
14. Axel L, Dougherty L (1989) MR imaging of motion with spatial modulation of magnetization. Radiology 171:841–845
15. Kuetting D, Sprinkart AM, Doerner J, Schild H, Thomas D (2015) Comparison of magnetic resonance feature tracking with harmonic phase imaging analysis (CSPAMM) for assessment of global and regional diastolic function. Eur J Radiol 84:100–107
16. Onishi T, Saha SK, Ludwig DR et al (2013) Feature tracking measurement of dyssynchrony from cardiovascular magnetic resonance cine acquisitions: comparison with echocardiographic speckle tracking. J Cardiovasc Magn Reson 15:95
17. Kempny A, Fernández-Jiménez R, Orwat S et al (2012) Quantification of biventricular myocardial function using cardiac magnetic resonance feature tracking, endocardial border delineation and echocardiographic speckle tracking in patients with repaired tetralogy of Fallot and healthy controls. J Cardiovasc Magn Reson 14:32
18. Hor KN, Baumann R, Pedrizzetti G et al (2011) Magnetic resonance derived myocardial strain assessment using feature tracking. J Vis Exp. https://doi.org/10.3791/2356
19. Collins JD (2015) Global and regional functional assessment of ischemic heart disease with cardiac MR imaging. Radiol Clin North Am 53:369–395
20. Onishi T, Saha SK, Delgado-Montero A et al (2015) Global longitudinal strain and global circumferential strain by speckle-tracking echocardiography and feature-tracking cardiac magnetic resonance imaging: comparison with left ventricular ejection fraction. J Am Soc Echocardiogr. https://doi.org/10.1016/j.echo.2014.11.018
21. Augustine D, Lewandowski AJ, Lazdam M et al (2013) Global and regional left ventricular myocardial deformation measures by magnetic resonance feature tracking in healthy volunteers: comparison with tagging and relevance of gender. J Cardiovasc Magn Reson 15:8
22. Lamacie MM, Thavendiranathan P, Hanneman K et al (2017) Quantification of global myocardial function by cine MRI deformable registration-based analysis: comparison with MR feature tracking and speckle-tracking echocardiography. Eur Radiol 27:1404–1415
23. Keller EJ, Fang S, Lin K et al (2017) The consistency of myocardial strain derived from heart deformation analysis. Int J Cardiovasc Imaging 33:1169–1177
24. Doesch C, Papavassiliu T, Michaely HJ et al (2013) Detection of myocardial ischemia by automated, motion-corrected, color-encoded perfusion maps compared with visual analysis of adenosine stress cardiovascular magnetic resonance imaging at 3 T: a pilot study. Invest Radiol 48:678–686
25. Jolly MP, Jordan JH, Meléndez GC, McNeal GR, D'Agostino RB Jr, Hundley WG (2017) Automated assessments of circumferential strain from cine CMR correlate with LVEF declines in cancer patients early after receipt of cardio-toxic chemotherapy. J Cardiovasc Magn Reson 19:59
26. Osman NF, McVeigh ER, Prince JL (2000) Imaging heart motion using harmonic phase MRI. IEEE Trans Med Imaging 19:186–202
27. Castillo E, Osman NF, Rosen BD et al (2005) Quantitative assessment of regional myocardial function with MR-tagging in a multicenter study: interobserver and intraobserver agreement of fast strain analysis with harmonic phase (HARP) MRI. J Cardiovasc Magn Reson 7:783–791
28. Simpson RM, Keegan J, Firmin DN (2013) MR assessment of regional myocardial mechanics. J Magn Reson Imaging 37:576–599
29. Lu JC, Connelly JA, Zhao L, Agarwal PP, Dorfman AL (2014) Strain measurement by cardiovascular magnetic resonance in pediatric cancer survivors: validation of feature tracking against harmonic phase imaging. Pediatr Radiol 44:1070–1076
30. Hor KN, Gottliebson WM, Carson C et al (2010) Comparison of magnetic resonance feature tracking for strain calculation with harmonic phase imaging analysis. JACC Cardiovasc Imaging 3:144–151
31. Schuster A, Kutty S, Padiyath A et al (2011) Cardiovascular magnetic resonance myocardial feature tracking detects quantitative wall motion during dobutamine stress. J Cardiovasc Magn Reson 13:58
32. Schuster A, Stahnke VC, Unterberg-Buchwald C et al (2015) Cardiovascular magnetic resonance feature-tracking assessment of myocardial mechanics: Intervendor agreement and considerations regarding reproducibility. Clin Radiol 70:989–998
33. Barreiro-Pérez M, Curione D, Symons R, Claus P, Voigt JU, Bogaert J (2018) Left ventricular global myocardial strain assessment comparing the reproducibility of four commercially available

CMR-feature tracking algorithms. Eur Radiol. https://doi.org/10.1007/s00330-018-5538-4

34. Hor KN, Wansapura J, Markham LW et al (2009) Circumferential strain analysis identifies strata of cardiomyopathy in Duchenne muscular dystrophy: a cardiac magnetic resonance tagging study. J Am Coll Cardiol 53:1204–1210
35. Feisst A, Kuetting DLR, Dabir D et al (2018) Influence of observer experience on cardiac magnetic resonance strain measurements using feature tracking and conventional tagging. Int J Cardiol Heart Vasc 18:46–51
36. Shehata ML, Cheng S, Osman NF, Bluemke DA, Lima JA (2009) Myocardial tissue tagging with cardiovascular magnetic resonance. J Cardiovasc Magn Reson 11:55
37. Venkatesh BA, Donekal S, Yoneyama K et al (2015) Regional myocardial functional patterns: quantitative tagged magnetic resonance imaging in an adult population free of cardiovascular risk factors: the multi-ethnic study of atherosclerosis (MESA). J Magn Reson Imaging 42:153–159